

Towards Classifying Histopathological Microscope Images As Time Series Data

Sungrae Hong^{○1}, Hyeongmin Park², Youngsin Ko³, Sol Lee¹, Bryan Wong¹, Mun Y Yi^{1*}

¹Grauate School of Data Science, KAIST, Daejeon, South Korea

²Department of Industrial Engineering, KAIST, Daejeon, South Korea

³Seegene Medical Foundation, Seoul, South Korea



Session 1 - 68
Poster No. (1571081670)

INTRODUCTION

✓ Background

- Cancer remains a leading cause of death worldwide, prompting the deep-learning based computer vision community to develop various models to address this critical issue [1].
- However, we note that the deep learning community has neglected microscopy images, which have significant practical advantages over scanned images. Specifically, nearly every existing research has been conducted on scanner-based images [2]. Microscopes are significantly more affordable than scanners thereby offering significantly different accessibility to patients in third-world nations [3].

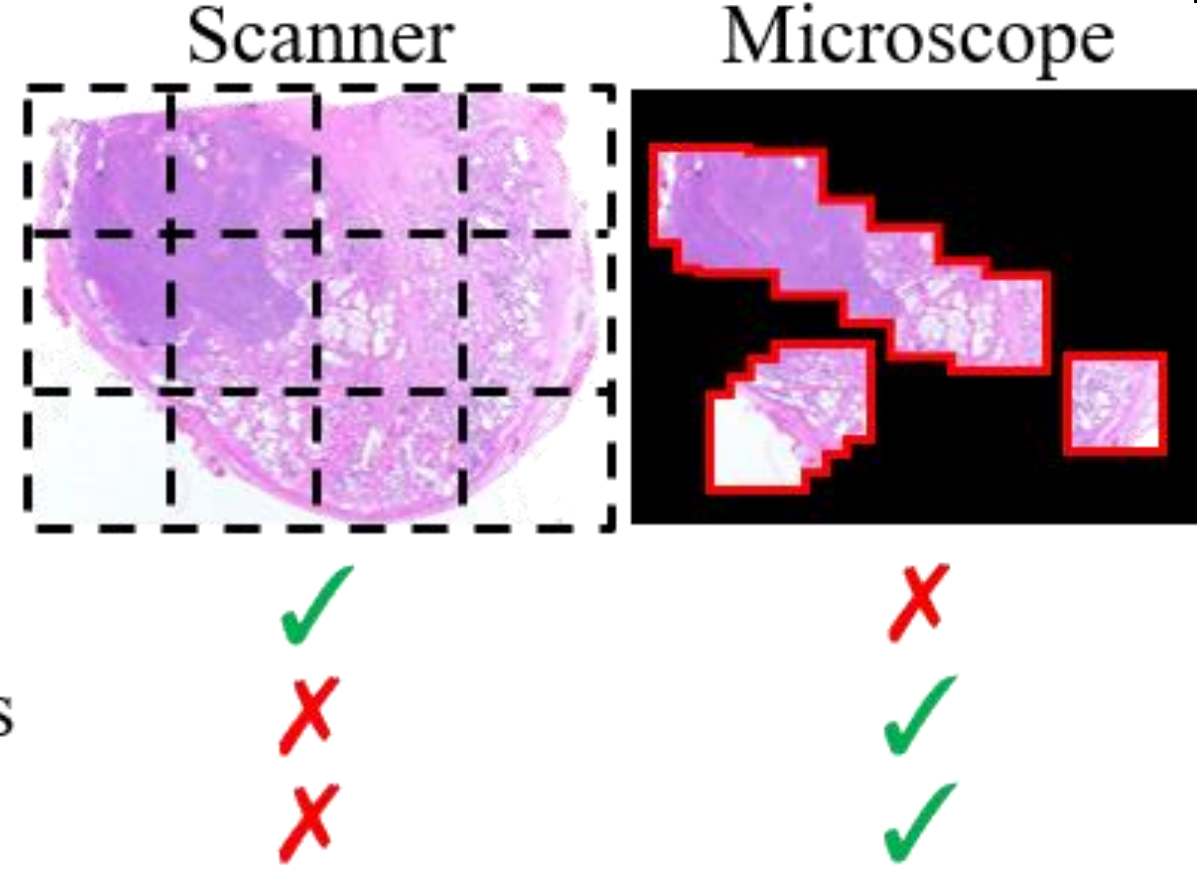


Fig. 1. denotes an image patch acquired by the scanner and a region captured by a microscope. Microscopy images are composed of overlapping sequences manually captured by domain experts

- ArbitraryLocations**: Microscopic images are periodically produced, making it impossible to accurately capture the coordinates of where the produced images were acquired.
- InconsistentLength**: The number of images captured per slide varies due to the automatic image acquisition process.
- Duplications**: The image acquisition process often results in a large number of redundant images.
- WeakLabel**: The absence of a whole-view, hundreds of images produced, make it very difficult for experts to annotate each images separately.

METHOD

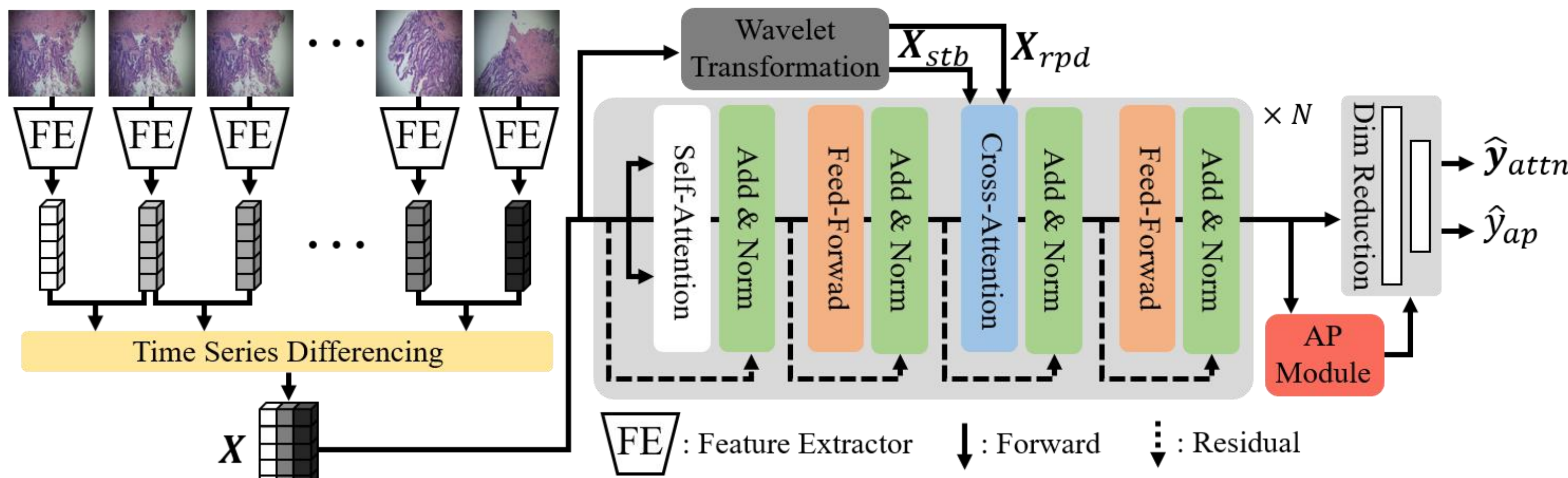


Fig. 2. Overall Framework

✓ Data processing

$$\Delta(x_i, x_{i+1}) = \|x_{i+1} - x_i\|_2^2 \quad (1)$$

- Time series differencing** We extract a feature sequence $X = \{x_i \in \mathbb{R}^d | i = 1, 2, \dots, n\}$ using pretrained extractor. We applied time series differencing to remove duplications (**Equation 1**).
- Wavelet transformation** Experts often capture narrow regions, causing similar symptoms to be filmed repeatedly. On the other hand, they occasionally move the slide glass to acquire images from entirely different regions. To mimic this pattern, we employ Wavelet transformation

✓ Attention module

$$\text{Attention}(Q, K, V) = \text{sigmoid}\left(\frac{QK^T}{\sqrt{d_k}}\right)V \quad (2)$$

$$\text{CrossAttention} = \lambda_{stb} \cdot \text{Attention}(Q, K_{stb}, V_{stb}) + \lambda_{rpd} \cdot \text{Attention}(Q, K_{rpd}, V_{rpd}) \quad (3)$$

- We used self-attention module for input sequence and corss-attention for X_{stb}, X_{rpd} .

✓ Attention Pooling (AP) module

$$P = \sum_{i=1}^n a_i x_i \in \mathbb{R}^d \quad (4)$$

$$a_i = \frac{\exp\{w^T(\tanh(A_t x_i) \odot \text{sigmoid}(A_s x_i))\}}{\sum_{j=1}^n \exp\{w^T(\tanh(A_t x_j) \odot \text{sigmoid}(A_s x_j))\}} \quad (5)$$

- This module aggregates sequence into a point prediction.

✓ Objective functions

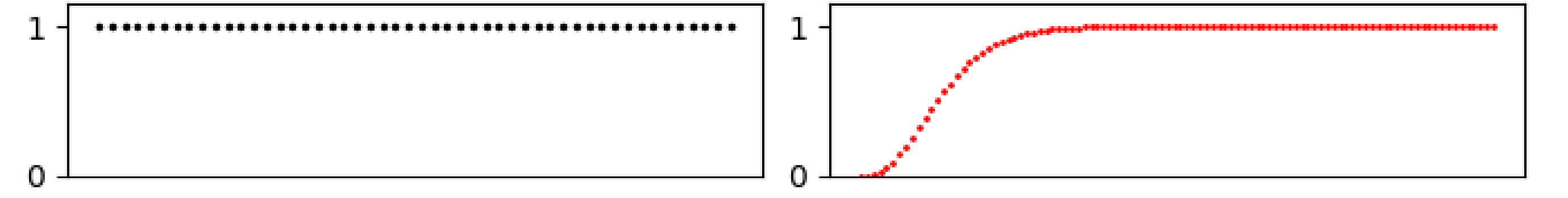


Fig. 4. Static target and proposed implicit target.

$$\mathcal{L}_{dtw} = \|D(\hat{y}_{attn}, y_l) - D(y_{ideal}, y_l)\|_1 \quad (6)$$

$$\mathcal{L}_{align} = \|\arg\max_{C_i \in \{C_1, \dots, C_n\}}(\hat{y}_{attn}) - \arg\max_C(\hat{y}_{ap})\|_1 \quad (7)$$

$$\mathcal{L} = \lambda_{dtw} \mathcal{L}_{dtw} + \lambda_{ap} \mathcal{L}_{ap} + \lambda_{align} \mathcal{L}_{align} \quad (8)$$

- The algorithm maps dynamic-length sequences closer to pre-defined target sequence. Because this is non-differentiable dynamic programming, we leverage the novel solution, Soft-DTW [4] $D(\cdot, \cdot)$.
- we propose using the cumulative distribution function of a Beta(3,20) as an implicit target to address the weakly supervised nature of our image sequences (**Fig. 4**). It is grounded in the empirical observation that experts find it challenging to capture regions exhibiting symptoms in a first frame due to the manual, high-zoom nature of the microscope.

EXPERIMENT

✓ Settings

	Magnitudes	n(Images)		n(Cases)		Average Images/Case	
		N	M	N	M	N	M
BreakHis	40×	652	1,370			27	24
	100×	644	1,437	24	58	27	25
	200×	623	1,390			26	24
	400×	588	1,232			15	21
Anonymous-Center	40×, 100×, 200×	52,076	84,100	492	423	106	199

Table 1. Dataset description. N and M indicates normal and malignant respectively.

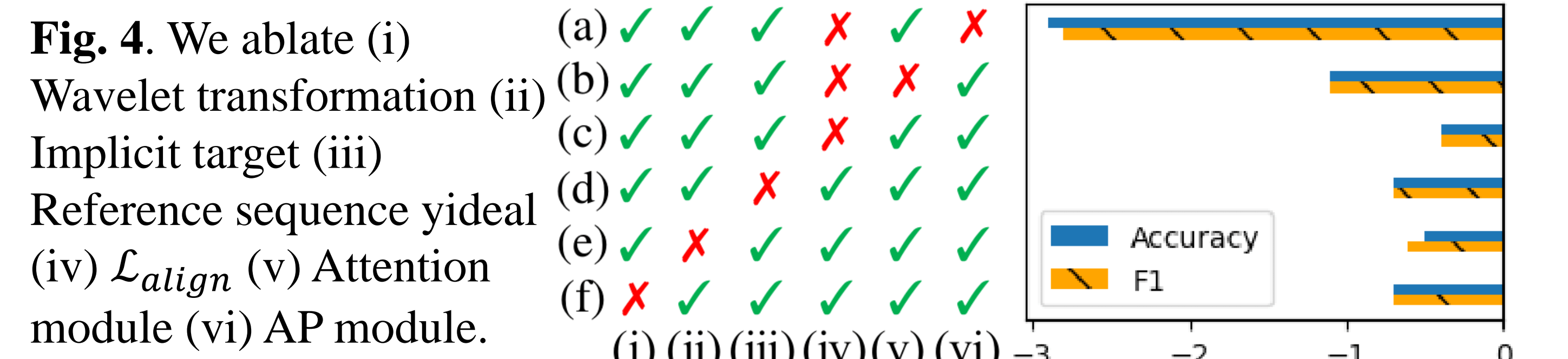
✓ Quantitative results

		AnonymousCenter (n=186)		BreakHis (n=28)							
				40×		100×		200×		400×	
		F1	Accuracy	F1	Accuracy	F1	Accuracy	F1	Accuracy	F1	Accuracy
LSTM [12]		0.975	0.976	0.940	0.914	0.923	0.893	0.938	0.914	0.925	0.893
GRU [13]		0.978	0.980	0.916	0.879	0.945	0.921	0.933	0.907	0.927	0.900
Transformer [9]		0.981	0.983	0.928	0.900	0.943	0.921	0.932	0.907	0.949	0.929
ABMIL [14]		0.982	0.984	0.891	0.850	0.913	0.871	0.911	0.871	0.904	0.857
TransMIL [15]		0.977	0.978	0.941	0.914	0.924	0.893	0.918	0.886	0.924	0.893
Ours	AP	0.990	0.991	0.954	0.936	0.947	0.929	0.945	0.921	0.954	0.936
	DTW Distance	0.988	0.989	0.962	0.950	0.951	0.936	0.947	0.929	0.969	0.957
	KNN	0.990	0.991	0.954	0.936	0.952	0.936	0.953	0.936	0.970	0.957
	Voting	0.990	0.991	0.964	0.950	0.952	0.936	0.958	0.943	0.964	0.950

Table 2. Comparison results

- Various inference strategies** Our proposed method offers four inference strategies: \hat{y}_{ap} prediction, DTW distance between \hat{y}_{attn} and y_l , KNN using \hat{y}_{attn}^{train} and \hat{y}_{attn} , and a majority voting of them.
- Quantitative results** Our proposed method can predict the entire sequence without truncation and aggregate the entire sequence for a single prediction, combining the advantages of both approaches.

✓ Ablation study



We present combinations of ablations from (a) to (f) and plot the performance decreases compared to the fully equipped model.

CONCLUSION

- We propose a novel framework that treats microscopic image sequences as time-series data. By employing various inference strategies and a voting mechanism, we achieved superior results.

REFERENCES: [1] Amelie Echle, Niklas Timon Rindtorff, Titus Josef Brinker, Tom Luedde, Alexander Thomas Pearson, and Jakob Nikolas Kather, "Deep learning in cancer pathology: a new generation of clinical biomarkers," British journal of cancer, vol. 124, no. 4, pp. 686-696, 2021. [2] Ruiwei Feng, Xuechen Liu, Jintai Chen, Danny Z Chen, Honghao Gao, and Jian Wu, "A deep learning approach for colonoscopy pathology wsi analysis: accurate segmentation and classification," IEEE Journal of Biomedical and Health Informatics, vol. 25, no. 10, pp. 3700-3708, 2020. [3] Yifan Zhang, Hanbo Chen, Ying Wei, Peilin Zhao, Jiezhong Cao, Xijuan Fan, Xiaoying Lou, Hailing Liu, Jinlong Hou, Xiao Han, et al., "From whole slide imaging to microscopy: Deep microscopy adaptation network for histopathology cancer image classification," in International conference on medical image computing and computer-assisted intervention. Springer, 2019, pp. 360-368. [4] Marco Cuturi and Mathieu Blondel, "Soft-dtw: a differentiable loss function for time-series," in International conference on machine learning. PMLR, 2017, pp. 894-903.

COMPLIANCE WITH ETHICAL STANDARDS: This study was performed in line with the principles of the Declaration of Helsinki. Approval was granted by the Ethics Review Board (SMF-IRB-2020-007) and (KAIST-IRB-22 335). Also, this research study was conducted retrospectively using human subject data made available in open access by [18]. Ethical approval was not required as confirmed by the license attached with the open access data. **Acknowledgement:** This research was supported by the Seegene Medical Foundation, South Korea, under the project "Research on Developing a Next Generation Medical Diagnosis System Using Deep Learning" (Grant Number: G01180115).

